CHARACTERIZING THE EFFECT OF TRANSVERSE STRAIN ON CARBON NANOTUBE BASED SENSING SKINS FOR STRUCTURAL HEALTH MONITORING

Sagar M. Doshi[1], Michael Coatney[2], Madison Weiss[1], Amit Chaudhari[1], Dae Han Sung[1], Erik T. Thostenson[1], Asha Hall[2]

1- Center for Composite Materials and Department of Mechanical Engineering, University of Delaware, Newark, Delaware
2 – Vehicle Technology Directorate, Army Research Laboratory, Aberdeen, Maryland

ABSTRACT

Due to the advancement in the science of processing and characterization of nanostructured materials, along with the industrial-scale production and decreasing cost of carbon nanotubes, their use in technologies as sensors and sensing skins is gaining popularity. With increasing Technology Readiness Levels (TRL) and field trials implemented by researchers, it is critical to characterize the sensing response of the carbon nanotube sensing skins under complex loading scenarios in order to simulate the real-life conditions. Typically, researchers describe the sensitivity (gage factor, GF) and sensing response of a carbon nanotube sensing skin based on the electrical resistance change and the longitudinal strain (ε_1), not taking into consideration the effect of transverse strain (ε_2) due to the Poisson's ratio of the material. Since the sensitivity of the sensor is dependent on the transverse strain, the sensitivity is affected by the properties of the substrate material. As a result, the calibration of the sensing skin is challenging. The principal objective of our research is to characterize the effect of transverse strain and develop a methodology to quantify the influence of transverse strain on the sensing response. The carbon nanotube-based sensing skins are manufactured using a scalable manufacturing technique and the effect of different loading scenarios on the sensing response are investigated. Carbon nanotubes are deposited on non-woven aramid fabrics with randomly oriented fibers and the resulting carbon nanotube-based sensing skin is bonded to steel and composite substrates which are subjected to flexural and axial loads to characterize the sensing response. A cruciform shaped specimen with a carbon nanotube sensor is tested using a biaxial testing machine and change in resistance under varying transverse loads is characterized. Key results indicate that the sensitivity of the carbon nanotube sensing skin is significantly affected by the transverse strain due to the Poisson effect which should be taken into consideration when calculating the gage factor or calibrating the sensors.

Keywords: Carbon Nanotubes, Strain Sensors, Structural Health Monitoring, Biaxial Testing, Poisson's Effect, Piezoresistive Sensors.

Corresponding author: Sagar M. Doshi – smdoshi@udel.edu

Copyright 2020. Used by the Society of the Advancement of Material and Process Engineering with permission.

SAMPE Virtual Conference Proceedings, 2020. Society for the Advancement of Material and Process Engineering – North America.

1. INTRODUCTION

Traditional techniques for monitoring the condition of civil infrastructure are often time consuming, inaccurate, expensive and ineffective. For example, a lot of bridges are still inspected at specific time intervals with manual markings made for fatigue cracks and other visible defects. These may often be unnoticed if they are in hard to reach areas or fatigue cracks initiate between the scheduled inspections. Multiple organizations have pointed out the deteriorating condition of the infrastructure in USA, for example, the American Society of Civil Engineers, in its report card (www.infrastructurereportcard.org) gave a grade of D+ for infrastructure. As a result, there exists a critical need for developing innovative sensors and sensing systems for effective structural health monitoring.

Typically strain gages can be used for monitoring the integrity of structures and the loads they are subjected to. A key challenge with the use of strain gages is that they are quasi point sensors may not be able to identify the damage if they are not in close vicinity or directly above the location of the damage. Field application of strain gages poses additional challenges with potential performance degradation over time due to environmental effects and wiring complexities. Researchers are working towards using acoustic emission sensors but their data analysis is involved and the interpretation of results is often not quantitative. Fiber optic sensors have an advantage over the point sensors and have been successfully used for distributed sensing [1,2], but there remain challenges with respect to compensation with temperature sensitivity, sensitivity for local strain and the ability to adequately cover the whole structure.

The rapid growth in the fundamental understanding, characterization techniques and the processing science in the field of nanotechnology in the last two decades has enabled specific tailoring and manipulation of nanomaterials. This has facilitated tremendous advancement in developing nanostructured hierarchical composites and textiles. Specifically, researchers have widely used carbon nanotubes due to their extraordinary properties for applications such as improving the mechanical properties of composites [3-5], self-sensing composites [6-8], energy harvesting composites [9,10], wearable strain sensors and flexible pressure sensors [11-15], sensing skin for structural health monitoring [16-18] and fatigue crack monitoring [19,20] and damage monitoring of joints [21].

With increasing focus on the research and development of carbon nanotube-based sensing skins, improving Technology Readiness Levels (TRL) and the rising number of field trials conducted, it is more important than ever to characterize the sensing response under different loading scenarios and to simulate real-life conditions addressing challenges such as calibration. For piezoresistive carbon nanotube-based sensors, researchers typically describe the sensitivity (gage factor GF) as the ratio of normalized change in electrical resistance ($\Delta R/R$) to longitudinal strain (ε_1), not taking into consideration the effect of transverse strain (ε_2).

$$Gage\ Factor\ (\boldsymbol{GF}) = \frac{\Delta R}{R} \times \frac{1}{\varepsilon_1}$$

While this works for sensors like metallic strain gages which are highly directional, but it is a significant source of inaccuracy when the transverse strain is not accounted for a carbon nanotube sensing skin which is sensitive to multi-axial strain. As a result, the sensor calibration is dependent on the substrate and its specific Poisson's ratio. For example, the sensor response when bonded to aluminum will be different than when bonded to steel or composite due to

different Poisson's ratio and the transverse strain due to it. Therefore, it is necessary to characterize the effect of transverse strain on the sensing response and investigate the sensor under different loading conditions.

In this research, a facile, scalable manufacturing technique of dip coating is used to create carbon nanotube-based sensing skin. The carbon nanotubes are deposited on a non-woven aramid fabric with randomly oriented fibers. The sensing response is characterized under different loading scenarios such as flexural and axial loading. The influence of Poisson effect (and the transverse strain due to it) on the sensing response is investigated by bonding the sensing skin to materials having different Poisson's ratio and on a cruciform shaped specimen loaded using a biaxial testing machine.

2. EXPERIMENTAL

2.1 Materials

A non-woven aramid fabric (20601 50 g/m^2, Technical Fiber Products) with fibers oriented in a random direction is used as a carrier of the carbon nanotubes for the sensing skin. A commercially available dispersion of carbon nanotubes (Aquacyl AQ0302, Nanocyl) is used for the dip coating process. A 2-part epoxy adhesive (Hysol 9309, Loctite) is applied for creating an insulating layer and bonding the sensing skin on substrates. The composite coupons and the cruciform specimen are manufactured using M40J unidirectional carbon fiber prepreg (Toray Carbon Fibers America). A flash dry silver paint (SPI supplies) and a 2-part conductive epoxy (Epoxies etc.) is used to connect the wires to reduce the contact resistance while measuring the electrical resistance.

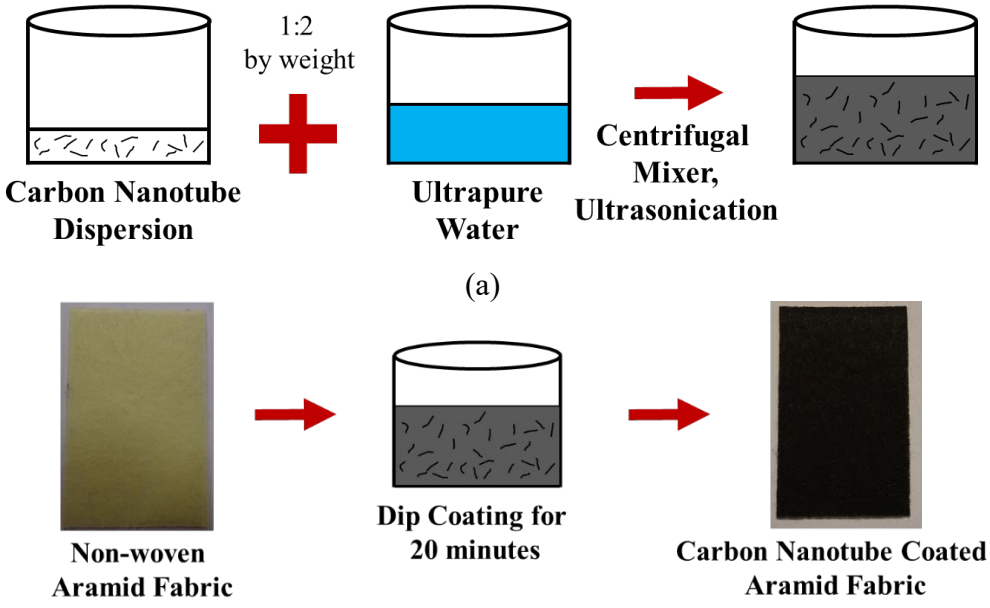


Figure 1. A schematic diagram of the manufacturing process for the carbon nanotube sensors. (a) shows the steps to create a uniform dispersion of carbon nanotubes and (b) shows the procedure followed in the dip coating process

2.2 Sensor Manufacturing using Dip Coating

The carbon nanotube-based sensing skins are created using a simple and easy to scale dip coating technique. The carbon nanotube dispersion, Aquacyl is diluted with ultrapure water in a ratio of 1:2 by weight. The diluted dispersion is then mixed using a planetary centrifugal mixer (ARM-310, Thinky) for 150 seconds at 2000 rpm. An ultrasonic bath sonicator is used for 30 minutes and the aramid fabric is dip coated for 20 minutes following drying in a convection oven at 150 ºC for 30 minutes. A schematic of the sensor manufacturing process is shown in Figure 1. The length of the sensing skin is 62.5 mm (2.5 inches) and the width 18.75 mm (3/4 inches).

2.3 Specimen Manufacturing

The carbon nanotube sensing skin is bonded to different substrates such as steel coupons, composite coupons and a composite cruciform for different types of tests. A similar procedure is followed for manufacturing all kinds of specimens. The surface area where the carbon nanotube sensor will be bonded is sandblasted and cleaned with acetone. A thin layer of the Hysol adhesive is applied to create an insulating layer to prevent direct contact of the sensing layer to steel or composite and avoid the electrical shorting of the sensor. Once the adhesive layer is partially cured, the sensing layer is bonded using the same adhesive and cured in an oven at 85 ºC for 1 hour and pressure is applied using clamps. A schematic of the steel specimen is shown in Figure 2. The part of the sensing skin where electrodes will be applied is masked using tape to prevent the adhesive from seeping in. The electrodes are then painted using a flash dry silver paint and the lead wires are attached using a 2-part conductive silver epoxy.

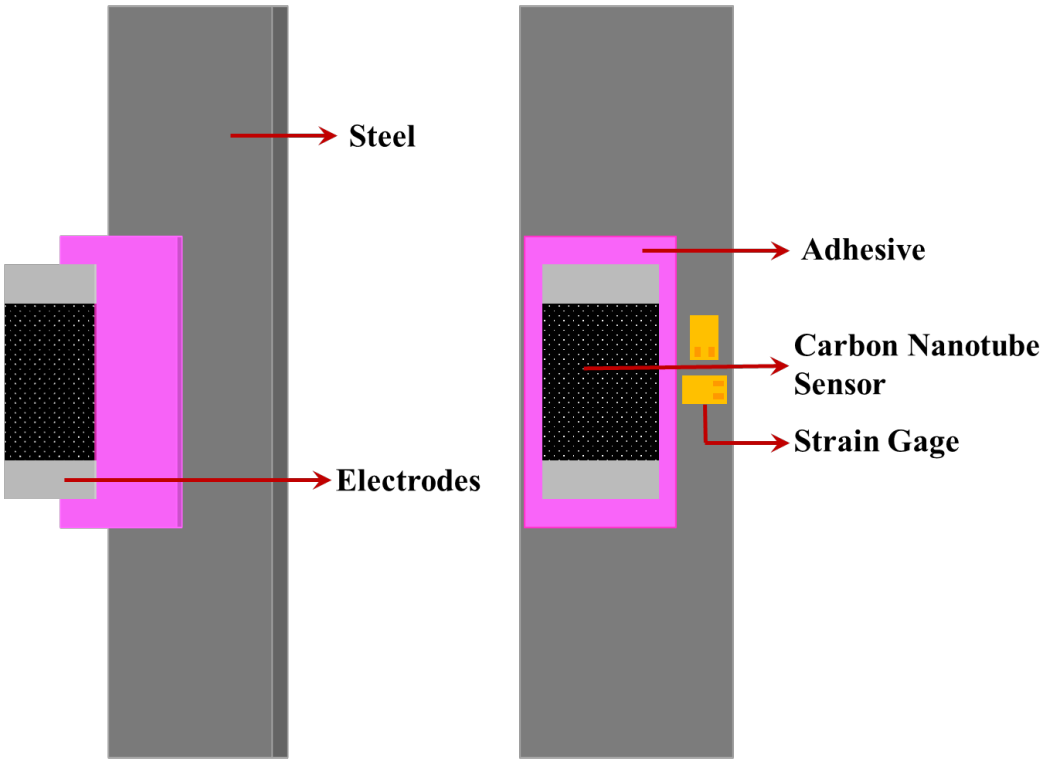
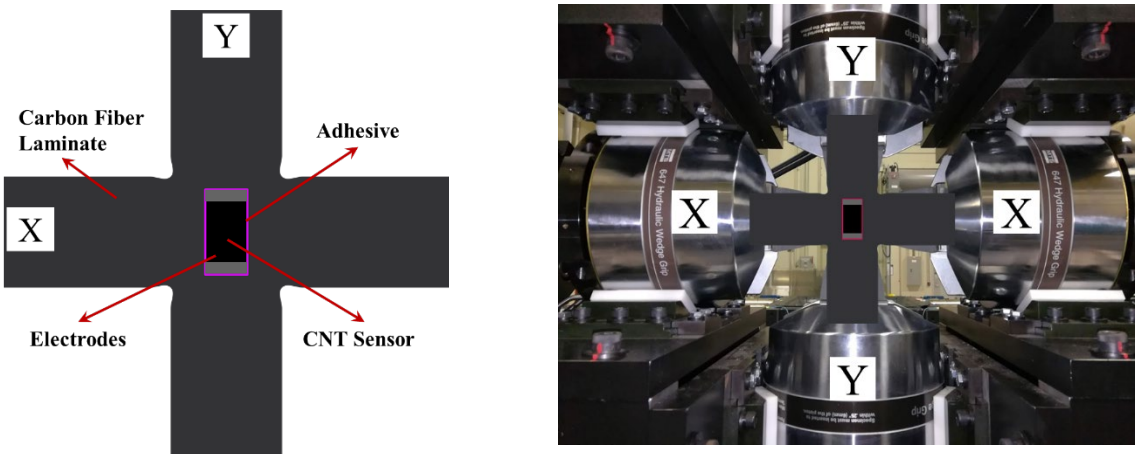


Figure 2. A schematic of the steel specimen with carbon nanotube sensing skin bonded.

2.4 Unidirectional Axial and Flexural Testing

The specimen is tested using a screw-driven mechanical load frame Instron 5985. For the flexural tests for steel specimens, a 4-point bending test is performed with the specimen supported at a distance of 300 mm (12 inches) and the load is applied at a distance of 50 mm (2 inches) from the center. A 4-point bending test is chosen so that the bending moment is constant within the loading area. The specimens are tested only in the elastic range to a strain of 0.1%. The maximum load in the axial test is 60 kN and the flexural test is 1.5 kN so that the specimens are subjected to similar strain levels of ~0.1%.

2.5 Biaxial Testing



(a) (b)

Figure 3 (a) A schematic illustration of the cruciform specimen with the carbon nanotube sensor and (b) a photograph of the biaxial testing machine with the schematic of the specimen overlaid showing the orientation of the sensor with respect to the machine Y and X axes.

The biaxial composite specimens are manufactured with a ply layup of $[0_4/90_4]_s$ with a total of 16 plies. A temperature of 135 ºC and pressure of 296 kPa is used for curing the composite in an autoclave for 120 minutes. The cruciform specimen is waterjet cut from a square laminate to dimensions as described by Skinner *et al.* [22] to have a uniform strain field in the center of the specimen. A schematic of the cruciform specimen is shown in Figure 3(a). The specimen is tested using an MTS planar biaxial servohydraulic testing machine (Figure 3(b)). This load frame is instrumented with 6 independent actuators. The maximum capacity of the load cell is 100 kN in the Y and X directions and 1100 N-m for a torsional load. Our specimen with the carbon nanotube sensor is was subjected to an in-plane load only. Maximum loads in the Y and X directions are varied to artificially create a different ratio of transverse strain/longitudinal strain. The maximum loads were limited to 9 kN to test the specimen in the elastic range with a maximum strain of just under 0.1%.

2.6 Electron Microscopy

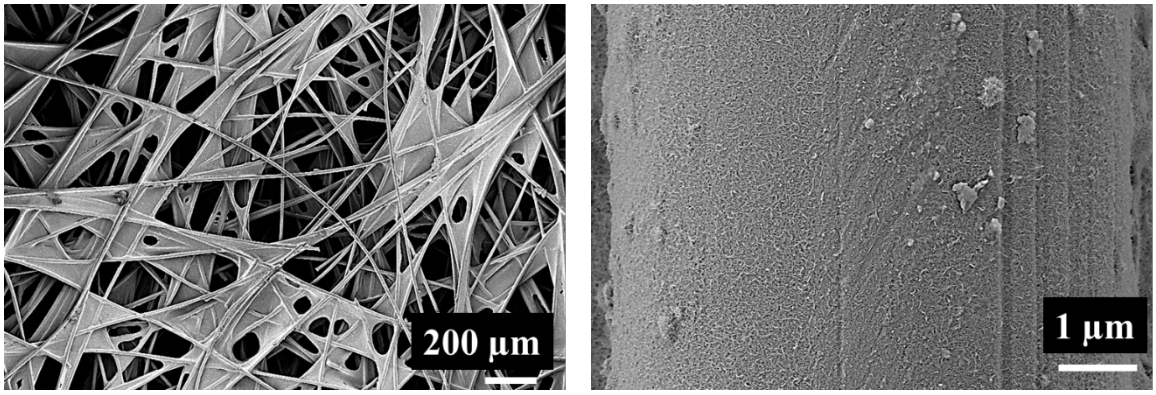
Scanning electron microscopy is conducted using a Zeiss Auriga 60 High Resolution Focused Ion Beam and Scanning Electron Microscope. An accelerating voltage of 3 kV and an SESI (Secondary Electron Secondary Ion) detector is used. The specimens are sputter coated with a

thin conductive layer of Pd/Au to minimize the charging using a sputter coating machine (Denton Desk IV).

3. RESULTS

3.1 Carbon Nanotube Film Characterization using Electron Microscopy

Figure 4 shows the scanning electron micrographs of the carbon nanotube-based sensing skin. The non-woven aramid fibers act as a carrier for the carbon nanotubes and create the backbone structure on which the nanotube forms a percolating conductive network. Figure 4(a) is a low magnification image showing the microstructure of the non-woven aramid fabric and the randomly oriented fibers in it. The binder used by the manufacturer to create the fabric forms web like structures between some fibers and is also coated with carbon nanotubes. Figure 4(b) shows a high magnification image of a fiber within the non-woven fabric with a uniform coating of carbon nanotubes. The carbon nanotubes are deposited on the entire fiber and on all the fibers within the fabric. It is due to this homogenous coating; the nanotubes are able to form a conductive network that enables piezoresistive sensing.



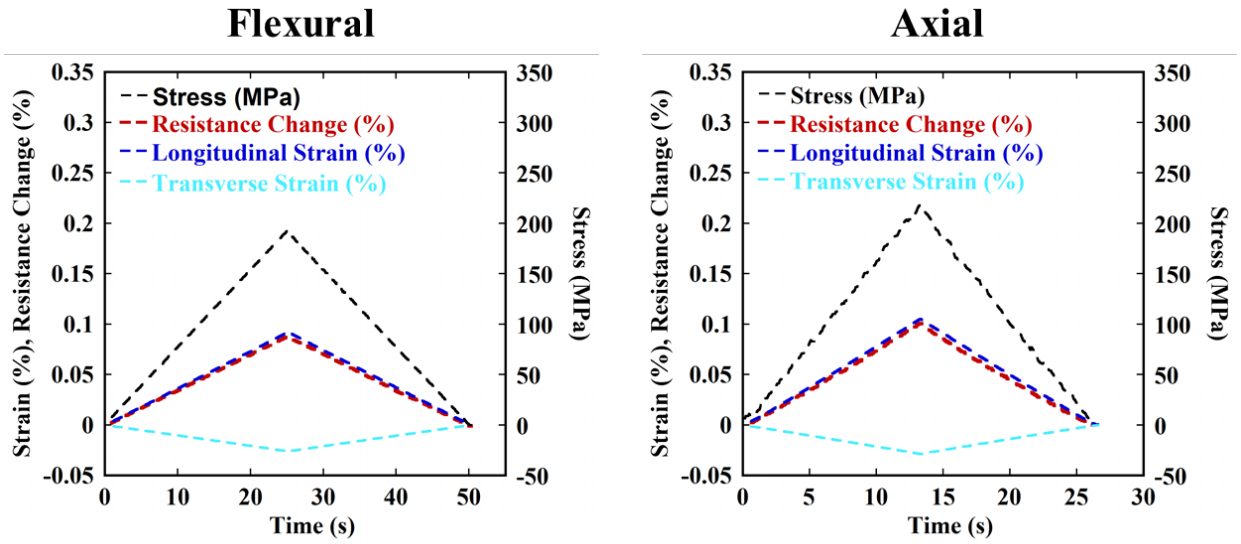
(a) (b)

Figure 4. Scanning electron micrographs of the carbon nanotube coated sensing skin. (a) Low magnification image showing the randomly oriented fibers in the non-woven fabric with binder forming web like structures between fibers and (b) high magnification image showing one of the fibers in the fabric which is uniformly coated with carbon nanotubes.

3.2 Electromechanical Characterization under Flexural and Axial Loads

To characterize the sensing response of the carbon nanotube-based sensing skin under different types of loads, the sensing skin was bonded to a steel coupon that was subjected to axial and flexural loads. The maximum loads for each test were chosen so that the applied longitudinal strain on the sensors would be ~ 0.1%, significantly below the yield strain. Figure 5 shows the strain, resistance change and stress versus time response for the loading and unloading cycle for the flexural and axial bending. The load applied for the 4-point bending was 1.5 kN and the stress was calculated using the flexure formula. The applied load for the axial test was 60 kN and the stress was calculated by dividing the load by area. The effect of the thin sensing layer is neglected for these calculations.

Figure 5 shows that the sensing response is independent of the type of loading. The applied stress for both types of loading is ~200 MPa and the maximum strain measured in the longitudinal direction is ~0.1% for both. The maximum percentage change in resistance is about 0.9 % for each case. Since the applied load is in the elastic range, upon unloading there is no permanent change in electrical resistance.



(a) (b)

Figure 5. Strain, resistance change and stress response vs time for the steel specimen when subjected to (a) flexural loading or 4 point bending and (b) axial loading. The resistance response is very similar and not dependent on the type loading.

3.3 Influence of Poisson's Ratio on the Sensing Response using Different Composite Laminates

To understand the influence of the substrate's Poisson's ratio on the sensing response, the carbon nanotube-based sensing skin is glued to 0º and 90º composite coupons and loaded in axial tension. Figures 6(a) and 6(b) show the load, resistance change (%) and strain (%) for carbon nanotube sensing skins when glued to a 0º and 90º composite coupon respectively. The maximum strain for both specimens is about 0.11%. The applied load for 0º specimen is 3000 N and for 90º specimen is 250 N for the same longitudinal strain because the Young's modulus in the direction of the fibers (0º) is significantly higher than the transverse direction (90º).

Since the sensing skin is sensitive to strains in all directions, the transverse contraction due to the Poisson effect also contributes to the bulk electrical resistance change. The contraction in the direction perpendicular to the loading direction will cause a decrease in electrical resistance. Therefore, the total percentage of electrical resistance change measured is the sum of resistance change due to longitudinal strain (positive and roughly equal for both specimens) and transverse strain (negative for 0º specimen and negligible for 90º specimen as shown in Figure 6(c) and 6(d)). As a result, the total percentage change in resistance is significantly higher for the 90º specimen than the 0º specimen even though both the specimens are subjected to similar longitudinal strain.

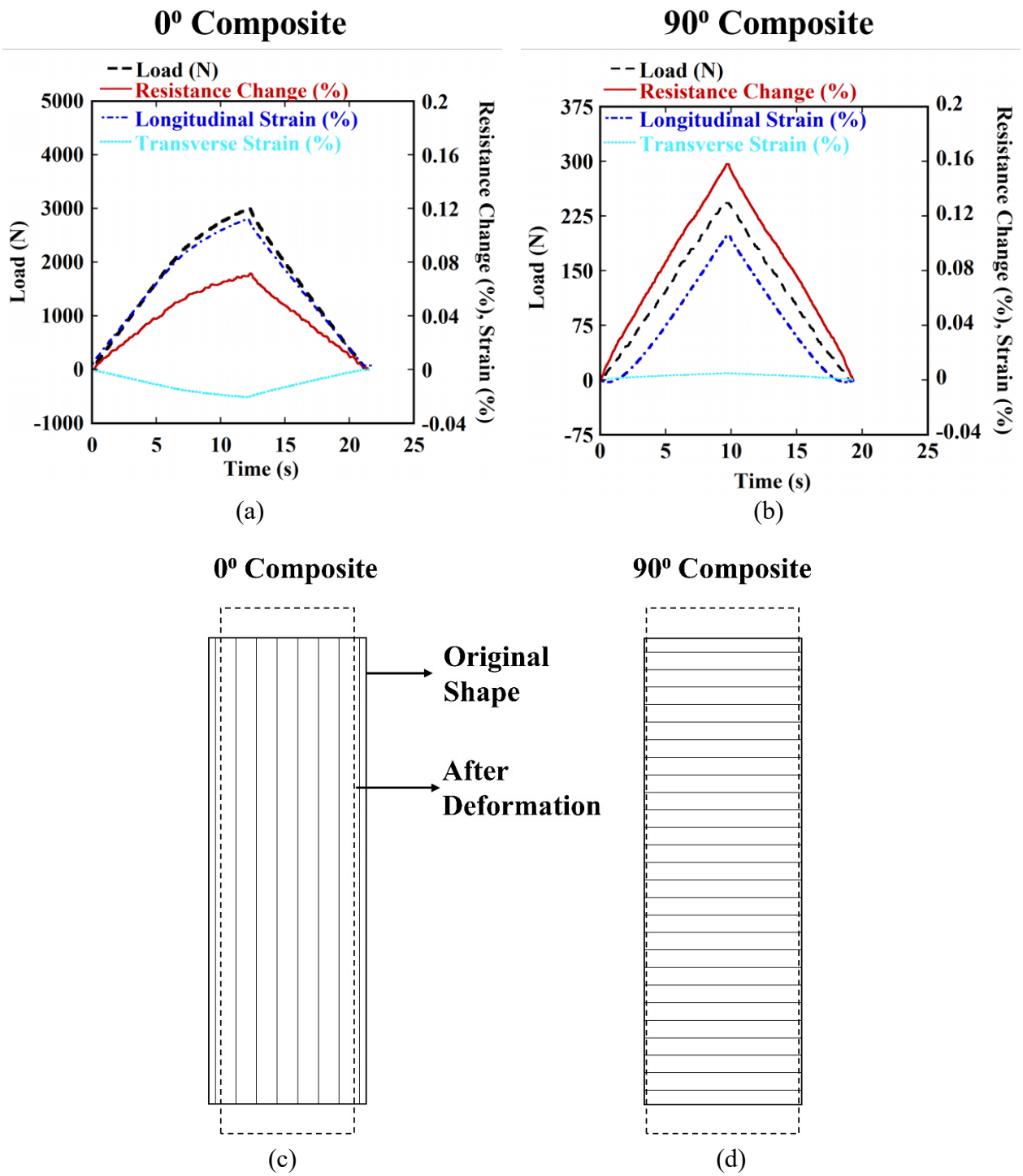


Figure 6. Load, resistance change and strain response vs. time when the carbon nanotube-based sensing skin is attached to (a) 0º composite coupon and (b) 90º composite coupon. For about the same maximum longitudinal strain, the percentage change in resistance is significantly greater for the 90º composite. (c) and (d) is a schematic showing the deformation of a typical 0º and 90º composite. The compression in 0º composite in transverse degree is due to a larger Poisson's ratio.

3.4 Sensing Response for a Cruciform Specimen using a Biaxial Testing Machine

To further investigate the effect of transverse strain on the sensing response, the carbon nanotube-based sensing skin is attached to a cruciform shaped specimen and tested using a biaxial testing machine. Three different types of loading conditions are applied. The load on the Y axis is +9 kN in all three cases whereas the load on the X axis (perpendicular to the direction of the sensor) is varied from -1.25 kN, +3 kN and to +9 kN. The loading curves for all three cases are shown in Figures 7(a), 7(b) and 7(c). The effective Poisson's ratio for each loading scenario is 0.14, -0.33 and -1, respectively. The strains in the Y and X direction for each loading case are shown in Figures 7(d), 7(e) and 7(f).

As observed in the previous experiments where the transverse strain plays a significant role in the total percentage resistance change and the sensitivity, in this case too, the load in the X direction (perpendicular to the sensor) plays a critical role. The percentage resistance change for three loading cases with decreasing Poisson's ratio is shown in figure 7(g), 7(h) and 7(i). In the first case, the load applied in the X direction was -1.25 kN compressive load. Therefore, the effective Poisson's ratio is positive 0.14. The total change in resistance is the sum of resistance change due to strain in the Y direction (positive) and X direction (negative). For the next two loading cases, the load in the X direction is 3 kN and 9 kN in tension. For these cases, the strain in both Y and X direction is positive and as a result the total resistance change is higher than the previous example where the load in X direction is compressive. A positive and higher effective Poisson's ratio indicates more compression and less total resistance change. A negative Poisson's ratio indicates tension in the transverse direction and results in a higher sensitivity and change in electrical resistance. For the three cases where Poisson's ratios are 0.14, -0.33 and -1 the total percentage resistance change is 0.09%, 0.13% and 0.2%, respectively.

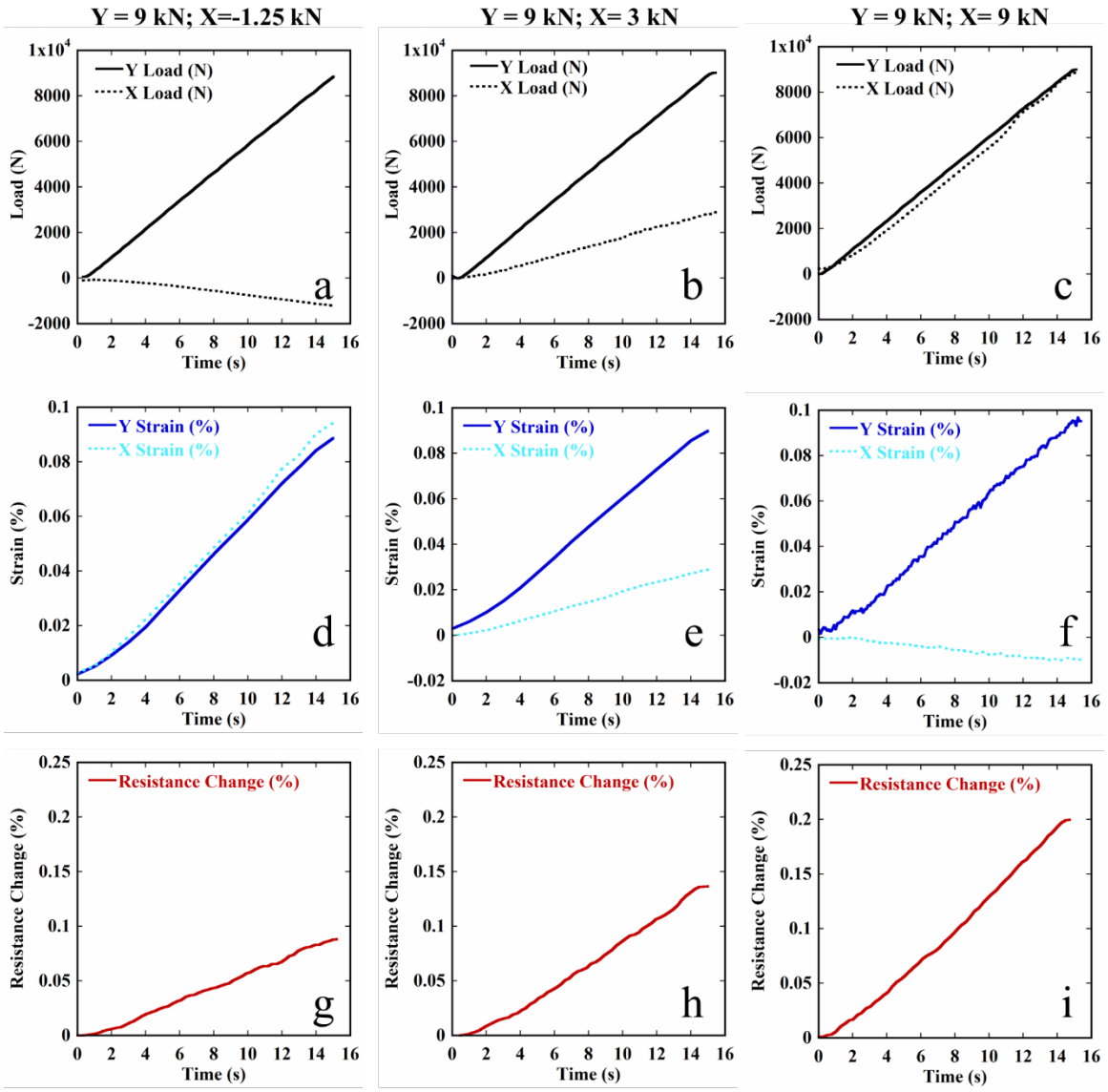


Figure 7. Load in Y and X direction vs. time for the three loading scenarios where Y = 9kN for all and (a) X= -1.25 kN, (b) X= +3 kN, (c) X= +9kN. Strain in Y and X direction vs. time for the three loading scenarios Y = 9kN for all and (d) X= -1.25 kN, (e) X= +3 kN, (f) X= +9kN. Percentage resistance change vs. time for the three loading scenarios Y = 9kN for all and (g) X= -1.25 kN, (h) X= +3 kN, (i) X= +9kN. The strain in transverse direction significantly affects the resistance response of the carbon nanotube sensing skin.

4. SUMMARY AND CONCLUSIONS

In summary, a scalable and facile manufacturing technique for carbon nanotube-based sensing skin is demonstrated. The sensing skin when attached to a steel coupon is subjected to axial and flexural loads and the resistance response is very similar when subjected to the same amount of longitudinal strain. This shows that the sensing response of the carbon nanotube sensor is independent of the type of load applied. Unlike a metallic strain gage, the carbon nanotube sensor is not directional and sensitive to deformation in all directions. As a result, the sensitivity of the sensor is significantly affected by Poisson's ratio of the substrate. When bonded to a 90º

composite (low Poisson's ratio) the resistance change is greater than when glued to 0º composite (high Poisson's ratio). Experiments were also conducted by attaching the sensor to a cruciform shaped specimen and tested using a biaxial testing machine where the load in the transverse direction was varied and the resistance response was significantly different for each case. The sensitivity of the carbon nanotube-based sensing skin is significantly affected by the transverse strain due to the Poisson's ratio of the substrate material and should be taken into consideration when calibrating sensors for field applications.

5. ACKNOWLEDGMENTS

This study is part of a research project funded under the Federal Highway Administration's Exploratory Advanced Research Program, Award No. DTFH61-13-H-00010. Frank Jalinoos is the project manager and his support is much appreciated. Any opinions, findings, and conclusions or recommendations expressed in this publication are those of the authors and do not necessarily reflect the view of the Federal Highway Administration. Funding from the UNIDEL Foundation and Army Research Laboratory is also acknowledged. The authors would like to thank Dr. Siddhant Datta, Mechanical Engineering Department of Arizona State University for guidance in performing the cruciform tests. Key technical inputs from Dr. Jaret Riddick and Dr. Mark Bundy are acknowledged. A special thanks to Ms. Lavern Coleman for facilitating tests at the Army Research Laboratory.

6. REFERENCES

1. Bassil, Antoine, et al. "Distributed fiber optics sensing and coda wave interferometry techniques for damage monitoring in concrete structures." Sensors 19.2 (2019): 356. doi.org/10.3390/s19020356
2. Enckell, Merit, et al. "Evaluation of a large-scale bridge strain, temperature and crack monitoring with distributed fibre optic sensors." Journal of Civil Structural Health Monitoring 1.1-2 (2011): 37-46. doi.org/10.1007/s13349-011-0004-x
3. Coleman, Jonathan N., et al. "Small but strong: a review of the mechanical properties of carbon nanotube–polymer composites." Carbon 44.9 (2006): 1624-1652. https://doi.org/10.1016/j.carbon.2006.02.038
4. Kausar, Ayesha, Irum Rafique, and Bakhtiar Muhammad. "Review of applications of polymer/carbon nanotubes and epoxy/CNT composites." Polymer-Plastics Technology and Engineering 55.11 (2016): 1167-1191. https://doi.org/10.1080/03602559.2016.1163588
5. An, Qi, et al. "Tailored glass fiber interphases via electrophoretic deposition of carbon nanotubes: fiber and interphase characterization." Composites Science and Technology 166 (2018): 131-139. https://doi.org/10.1016/j.compscitech.2018.01.003
6. Doshi SM, Thostenson ET. Self-sensing carbon nanotube composites: processing and characterization. Multifunctionality of Polymer Composites: Challenges and New Solutions; 2015; Chapter 25, 752–84 https://doi.org/10.1016/C2013-0-13006-1
7. Nataraj, Latha, et al. "Early-Stage Damage Detection in Advanced Multifunctional Aerospace Composites Using Embedded Carbon Nanotubes and Flocked Carbon Fibers." Multidisciplinary Digital Publishing Institute Proceedings. Vol. 2. No. 8. 2018.

https://doi.org/10.3390/ICEM18-05386

8. Gao, Shang-lin, et al. "Glass fibers with carbon nanotube networks as multifunctional sensors." Advanced Functional Materials 20.12 (2010): 1885-1893. https://doi.org/10.1002/adfm.201000283
9. Sung, Dae Han, et al. "Characterization of thermoelectric properties of multifunctional multiscale composites and fiber-reinforced composites for thermal energy harvesting." Composites Part B: Engineering 92 (2016): 202-209. https://doi.org/10.1016/j.compositesb.2016.02.050
10. Hu, Renchong, et al. "Harvesting waste thermal energy using a carbon-nanotube-based thermo-electrochemical cell." Nano letters 10.3 (2010): 838-846. https://doi.org/10.1021/nl903267n
11. Doshi, Sagar M., and Erik T. Thostenson. "Thin and Flexible Carbon Nanotube-Based Pressure Sensors with Ultrawide Sensing Range." ACS sensors 3.7 (2018): 1276-1282. https://doi.org/10.1021/acssensors.8b00378
12. Jiang, Shuwen, et al. "An Ultra-wide Sensing Range and Highly Sensitive Flexible Pressure Sensor Based on Percolative Thin Film with Knoll-like Micro-structured Surface." ACS applied materials & interfaces (2019). https://doi.org/10.1021/acsami.9b02659
13. Zhang, Hao, et al. "Flexible and Pressure-Responsive Sensors from Cellulose Fibers Coated with Multiwalled Carbon Nanotubes." ACS Applied Electronic Materials 1.7 (2019): 1179-1188. https://doi.org/10.1021/acsaelm.9b00182
14. Doshi, Sagar M., et al. "Carbon Nanotube Coated Textile Sensors with Ultrahigh Sensitivity for Human Motion Detection" Proceedings of the IEEE Sensors Conference, Montreal, Oct 27th-30th, 2019.
15. Doshi, Sagar M., et al. "Carbon Nanotube Based Flexible Sensors for Human Motion Analysis." Proceedings of the American Society for Composites—Thirty-fourth Technical Conference. Atlanta, Sep 23rd-25th, 2019.
16. Ahmed, Shafique, et al. "Development of a novel integrated strengthening and sensing methodology for steel structures using CNT-based composites." Journal of Structural Engineering 143.4 (2016): 04016202. https://doi.org/10.1061/(ASCE)ST.1943-541X.0001697
17. Schumacher, Thomas, and Erik T. Thostenson. "Development of structural carbon nanotube–based sensing composites for concrete structures." Journal of Intelligent Material Systems and Structures 25.11 (2014): 1331-1339. https://doi.org/10.1177/1045389X13505252
18. Dai, Hongbo, et al. "Processing and characterization of a novel distributed strain sensor using carbon nanotube-based nonwoven composites." Sensors 15.7 (2015): 17728-17747. https://doi.org/10.3390/s150717728
19. Ahmed, Shafique, et al. "Integration of carbon nanotube sensing skins and carbon fiber composites for monitoring and structural repair of fatigue cracked metal structures." Composite Structures 203 (2018): 182-192.

https://doi.org/10.1016/j.compstruct.2018.07.005

20. Kwon, Dong-Jun, et al. "Damage sensing and fracture detection of CNT paste using electrical resistance measurements." Composites Part B: Engineering 90 (2016): 386-391. https://doi.org/10.1016/j.compositesb.2016.01.020
21. Ahmed, Shafique, et al. "Experimental and numerical investigation on the bond strength of self-sensing composite joints." International Journal of Adhesion and Adhesives 84 (2018): 227-237. https://doi.org/10.1016/j.ijadhadh.2018.03.014
22. Skinner, Travis, et al. "Fatigue damage behavior in carbon fiber polymer composites under biaxial loading." Composites Part B: Engineering (2019): 106942. https://doi.org/10.1016/j.compositesb.2019.106942